

1 **A Repeating Earthquake Catalog from 2003 to 2018 for**
2 **the Raukumara Peninsula, Northern Hikurangi**
3 **Subduction Margin, New Zealand**

4 **Laura Hughes¹, Calum J. Chamberlain¹, John Townend¹, Amanda M.**
5 **Thomas²**

6 ¹School of Geography, Environment and Earth Sciences, Victoria University of Wellington, PO Box 600,
7 Wellington 6140, New Zealand

8 ²Department of Earth Sciences, University of Oregon, Eugene, Oregon, USA

9 **Key Points:**

- 10 • 62 repeating earthquakes families were identified between 2003 and 2018 around
11 the Raukumara Peninsula
12 • Family focal mechanisms are consistent with both intra- and inter-plate faulting
13 • Timing of the repeating events coincide with previously identified slow-slip
14 events and locate at the edges of slow-slip patches

Corresponding author: Laura Hughes, hughes.lauragrace@gmail.com

Abstract

Repeating earthquakes provide a novel way of monitoring how stresses load faults between large earthquakes. To date, however, and despite the availability of long-duration, high-quality seismological datasets, little attention has been paid to tectonic repeating earthquakes in New Zealand. We develop a workflow and composite criterion for identifying repeating earthquakes in New Zealand, using data from the GeoNet permanent seismic network, and present New Zealand’s first decadal-scale repeating earthquake catalog. For events to be identified as repeating in this study, two or more events must have a normalized cross-correlation of at least 0.95 at two or more seismic stations, when calculated for 75% of the earthquake coda. By applying our composite criterion to seismicity around the Raukumara Peninsula, northern Hikurangi subduction margin, we have identified 62 repeating earthquake families occurring between 2003 and 2018, consisting of 160 individual earthquakes. These families have a magnitude range of M_W 1.5–4.5 and recurrence intervals of < 1–12 years. The repeating earthquake families identified in this study coincide with the location and timing of previously identified slow-slip events and tremor. However, the responses shown to slow-slip are not consistent within families or within regional groups.

Plain Language Summary

Repeating earthquakes are earthquakes that re-rupture the same fault patch thereby producing highly similar seismograms, and occur sporadically and in some cases periodically through time. In this study, we developed a methodological workflow and a criterion for identifying repeating earthquakes in New Zealand, using data from the GeoNet permanent seismic network. The criterion is similar to that used in previous repeating earthquake studies at plate boundary zones elsewhere, but is customized to the available data and earthquake sources of interest. We identified 62 repeating earthquake families, consisting of 160 individual earthquakes, which occurred between 2003 and 2018 around the Raukumara Peninsula, northeastern North Island. The location and timing of the repeating earthquake families coincide with those of previously identified slow-slip and tremor.

1 Introduction

Monitoring and interpreting how stresses load faults in the run-up to large earthquakes, and what impact this has on nucleation and rupture processes, remains a significant challenge in earthquake physics (e.g. Passelègue et al., 2020). Repeating earthquakes provide one means of monitoring these processes within the seismogenic portions of faults (Uchida et al., 2003). In New Zealand, little attention has been paid to repeating earthquakes, despite the availability of high-quality, long-duration seismological datasets. In this paper, we describe the construction and analysis of the first long-duration catalog of repeating earthquakes of tectonic origin in New Zealand.

1.1 Repeating earthquakes

Repeating earthquakes are identified primarily on the basis of their highly similar waveforms, observed at multiple stations, which imply similar hypocenters and focal mechanisms (e.g. Nadeau et al., 1994; Nadeau & Johnson, 1998; Uchida et al., 2003; Zhang et al., 2008; K. H. Chen et al., 2013; Naoi et al., 2015; Li et al., 2018; Senobari & Funning, 2019). Due to their similarities, it is hypothesized that repeating earthquakes represent the repeated rupture of the same strong asperity or fault patch (e.g. Nadeau & McEvilly, 1999; Uchida et al., 2003). Repeating earthquakes have been the subject of extensive research at several plate boundary zones, notably the Japan Trench (e.g. Hatakeyama et al., 2017; Uchida et al., 2003) and the San Andreas fault system (e.g.

63 Nadeau et al., 1994; Thomas et al., 2016; J. R. Williams et al., 2019; Abercrombie,
 64 Rachel E. and Chen, Xiaowei and Zhang, Jiewen, 2020), as well as China (e.g. Schaff
 65 & Richards, 2004), Taiwan (e.g. K. H. Chen et al., 2008), Costa Rica (e.g. Chaves
 66 et al., 2020; Yao et al., 2017), Greece (e.g. Mesimeri & Karakostas, 2018) and the
 67 Tonga–Kermadec Trench (e.g. Yu, 2013).

68 If, as hypothesized, repeating earthquakes represent repeated failure of the same
 69 fault patch, due to successive phases of loading and slip, then their magnitudes —
 70 or equivalently their stress-drops, assuming the same rupture area — and inter-event
 71 times will be interpretable in terms of stressing-rate. Furthermore, the interaction
 72 between repeating earthquakes within a family, between different families, and with
 73 nearby and distal seismic and aseismic phenomena may provide insights into fault
 74 properties (e.g. Marone et al., 1995) and changes in the surrounding stress field (e.g.
 75 Nadeau et al., 1995; Lui & Lapusta, 2016). The interaction between large earthquakes
 76 nearby and repeating earthquake families can also provide information about how
 77 stresses are loading the small asperities on which repeating earthquakes are assumed
 78 to be occurring (K. H. Chen et al., 2010, 2013; Wu et al., 2014). Repeating earthquakes
 79 have also been recorded during episodes of slow slip (Kato et al., 2012; Shaddock &
 80 Schwartz, 2019), and have been used as a proxy to monitor aseismic creep prior to
 81 large earthquakes (e.g. Mavrommatis et al., 2015; Kato et al., 2012).

82 Fault slip-rates can be estimated from repeating earthquake observations using
 83 either the recurrence interval and seismic moments of the repeating earthquakes (e.g.
 84 Mavrommatis et al., 2015; Nomura et al., 2017) or the average seismic moment of the
 85 family (e.g. Nadeau & Johnson, 1998; Uchida et al., 2003). Slip-rates can then be
 86 determined by dividing the estimated slip by the repeating earthquake family dura-
 87 tion. An extension of this allows variable slip-rates to be modeled to show changes
 88 in the amount and rate of slip on the fault patches where repeating earthquakes are
 89 occurring (Mavrommatis et al., 2015; Nadeau & Johnson, 1998; Nomura et al., 2017).
 90 Changes in slip-rate recorded by repeating earthquake families have been observed in
 91 the lead up to, and/or following, large earthquakes (Mavrommatis et al., 2015; No-
 92 mura et al., 2017). Hence, our work provides the first step to potentially monitoring
 93 changes in slip-rates around the plate boundaries of New Zealand.

94 1.2 Tectonic setting

95 The Hikurangi Subduction Margin accommodates convergence of the Australian
 96 and Pacific Plates and runs the length of the North Island of New Zealand (Clark
 97 et al., 2019), posing the largest seismic hazard for New Zealand (Clark et al., 2019).
 98 Due to the risk of great earthquakes ($M \geq 8$) occurring along this margin, extensive
 99 research has been undertaken to examine and quantify the associated hazard and risks
 100 (Clark et al., 2019, and references therein). Convergence rates vary from 32 mm/yr in
 101 the south, to 54 mm/yr in the north. Interface coupling also varies along the margin,
 102 with the interface locked to ~ 35 km depth in the south but only to ~ 10 km depth in
 103 the north (Wallace et al., 2009; Wallace, 2020).

104 The Raukumara Peninsula lies above the northern Hikurangi Subduction Margin
 105 in the northeast of New Zealand’s North Island (Figure 1). Here the Pacific Plate is
 106 subducting beneath the Australian Plate with convergence rates at the trench rang-
 107 ing from ~ 47 mm/yr at the southern extent of the Peninsula, to ~ 57 mm/yr to the
 108 north (Figure 1) (Wallace et al., 2012). Beneath the eastern edge of the Raukumara
 109 Peninsula, the plate interface is inferred to lie at ~ 12 – 15 km and it progressively deep-
 110 ens to ~ 50 km beneath the western edge (C. A. Williams et al., 2013). Upper plate
 111 faults in the North Island Dextral Fault Belt in the overriding Australian Plate ac-
 112 commodate much of the right-lateral strike-slip component of the Australia-Pacific
 113 relative plate motion (Figure 1) (Beanland, 1995; Wallace et al., 2004; Nicol & Wal-

114 lace, 2007). Reverse faults have been imaged offshore from the Raukumara Peninsula
115 and accommodate part of the convergent component of relative plate motion (Barnes
116 et al., 2010; Mountjoy & Barnes, 2011; Litchfield et al., 2020).

117 These tectonic components exhibit a wide range of transient seismic phenomena
118 throughout the Raukumara Peninsula and surrounding region (Wallace et al., 2009),
119 including moderate- to large-magnitude earthquakes ($M \leq 7.2$) (Francois-Holden et al.,
120 2008; Koulali et al., 2017; Warren-Smith et al., 2018), repeated episodes of shallow and
121 deep slow-slip (e.g. Douglas et al., 2005; Wallace & Beavan, 2010; Wallace et al., 2012,
122 2016, 2018; Wallace, 2020), tectonic tremor (Todd & Schwartz, 2016; Todd et al.,
123 2018), triggered seismicity (Delahaye et al., 2009), and recently documented burst-
124 type repeating earthquakes (Shaddock & Schwartz, 2019) (Figure 1). Several large
125 earthquakes have occurred across the region in the last century. Of particular note are
126 two M_W 7.2 tsunamigenic earthquakes that occurred in March and May of 1947 off the
127 coast of Gisborne and Tokomaru Bay (Bell et al., 2014; Doser & Webb, 2003), a normal-
128 faulting intraslab M_W 6.6 event offshore from Gisborne in December 2007 (Francois-
129 Holden et al., 2008), and the M_W 7.1 Te Araroa earthquake of September 2016 (Koulali
130 et al., 2017; Warren-Smith et al., 2018). These larger events appear to often involve
131 interactions with other seismic phenomena: for instance, the Te Araroa earthquake
132 was preceded by slow-slip events (Koulali et al., 2017; Warren-Smith et al., 2018).

133 Repeated slow-slip is a common occurrence along the eastern edge of the Rauku-
134 mara Peninsula (Wallace, 2020). At the northern end of the Hikurangi Subduc-
135 tion Margin, slow-slip events (SSEs) have typical recurrence intervals of 18 to 24
136 months (e.g. Douglas et al., 2005; Wallace & Beavan, 2010; Wallace et al., 2016).
137 The equivalent moment magnitudes of these SSEs are M_W 6.3 to 7.2, and they typi-
138 cally occur at depths of less than 15 km (Koulali et al., 2017; Wallace & Beavan, 2010).
139 SSEs along most of the the Hikurangi Subduction Margin were triggered by the 2016
140 M_W 7.8 Kaikōura earthquake in the weeks to months that followed (Wallace et al.,
141 2018).

142 SSEs have been observed simultaneously with both tremor (e.g. Todd & Schwartz,
143 2016; Todd et al., 2018) and distinctive microseismicity (Delahaye et al., 2009), at
144 the northern Hikurangi Subduction Margin. Todd and Schwartz (2016) and Todd et
145 al. (2018) concluded that the northern Hikurangi SSEs tend to be accompanied by
146 tremor, which typically occurs down-dip of the geodetically determined slip patch,
147 and typically occur towards the end of the SSE and afterwards. Tremor has been most
148 commonly observed during the larger-magnitude SSEs around the Gisborne area, but
149 has also been documented during smaller SSEs further north in the vicinity of Tolaga
150 Bay and Puketiti. However, tremor associated with offshore SSEs is often difficult to
151 detect using New Zealand’s entirely land-based national seismic network (Delahaye et
152 al., 2009; Todd & Schwartz, 2016; Todd et al., 2018), complicating interpretation of
153 its relationship to SSEs.

154 Recently, “burst-type” repeating earthquakes have been identified near the Rauku-
155 mara Peninsula following the 2014 Gisborne SSE (Figure 1; Shaddock & Schwartz,
156 2019). These repeating earthquakes were inferred to occur on an upper-plate fracture
157 network above a subducting seamount, and were only observed to be active for a short
158 time period (approximately seven weeks; Shaddock & Schwartz, 2019). We note that
159 such “burst-type” repeating earthquakes were detected using less stringent waveform
160 similarity criteria than employed in most other repeating earthquake studies referred
161 to above (cf. Uchida & Bürgmann, 2019), and may not represent repeated slip of
162 exactly the same asperity. Other than the study by Shaddock and Schwartz (2019)
163 of burst-type repeating earthquakes accompanying the 2014 Gisborne SSE, no long-
164 duration analyses of tectonic repeating earthquakes have been undertaken around the
165 Raukumara Peninsula.

1.3 Repeating earthquake identification around the Raukumara Peninsula

In this paper, we describe the construction and interpretation of the first long-duration tectonic repeating earthquake catalog in New Zealand. We have focused our search for repeating earthquakes on the Raukumara Peninsula, due to the high levels of seismicity observed in the region and the large number of previously documented interactions between seismic and aseismic deformation phenomena occurring in the northern Hikurangi Subduction Margin (Wallace, 2020).

The first step in our analysis has been to develop and test a workflow and composite detection criterion for identifying repeating earthquakes in the New Zealand context using data from the GeoNet network. Waveform cross-correlation is the most commonly used method for identifying repeating earthquakes (Nadeau et al., 1994; Senobari & Funning, 2019; Uchida & Bürgmann, 2019). Cross-correlations are calculated for candidate pairs of earthquakes that are within a given hypocentral distance of one another, with the events being identified as repeating if they have a normalized cross-correlation exceeding some threshold (commonly 0.90 to 0.95) at multiple seismic stations (e.g. Nadeau et al., 1995; Nomura et al., 2017). While the majority of studies follow this general approach, each study has adapted components of the detection criteria to local conditions and requirements, including the length of the waveforms used to calculate the cross-correlation, the number of stations required, the filtering applied to the waveforms, and the threshold imposed to cope with particular geometries and data quality (e.g. Nadeau & Johnson, 1998; Bohnhoff et al., 2017).

2 Methods

2.1 Dataset and initial clustering

We constructed our catalog of repeating earthquakes starting with the GeoNet seismicity catalog from 1 January 1987 to 26 July 2019 (as downloaded from the GeoNet International Federation of Digital Seismograph Networks (FDSN) service (<https://www.geonet.org.nz/data/tools/FDSN>) on 26 July 2019). We downloaded waveform data from the GeoNet FDSN service using ObsPy (Krischer et al., 2015) for all broadband and short-period stations and channels represented by the cataloged picks. We first clustered the entire GeoNet catalog of 570,671 earthquakes throughout New Zealand based on inter-event separation and multi-station averaged inter-event cross-correlation. This initial clustering was conducted with a low cross-correlation threshold (0.75) and relatively large inter-event separation (30 km) to allow for location uncertainties. Note that throughout this paper the term “cross-correlation” refers to fully normalised cross-correlation.

In this initial step, cross-correlations were computed on the vertical channels of 2–15 Hz instrument-response-corrected bandpassed data resampled to 50 Hz beginning 2 s before the P-pick and of 6 s duration. Single-station correlations were allowed to shift by ± 1.5 s to allow for pick uncertainty, and the maximum cross-correlations for each station were averaged to generate a mean inter-event cross-correlation. Cross-correlations were only computed for pairs of events with hypocentral separations of less than 30 km to reduce computational demands. To cope with multiple possible groupings, we used a hierarchical clustering approach, as implemented in SciPy (Virtanen et al., 2020) and applied using EQcorrscan (Chamberlain et al., 2018) to assign earthquakes to clusters of potentially repeating events (herein termed “families”).

The purpose of this initial clustering step was to reduce the size of the dataset and allow efficient testing of the parameters used to define repeating earthquakes in the Raukumara Peninsula study region. Based on this initial clustering, we extracted earthquakes within the region between -37.2 and -39.2 degrees latitude and 177.2

216 and 179.7 degrees longitude for further analysis. This region contained 133 possible
 217 repeating earthquake families. For each of these 133 possible families, we conducted
 218 manual phase-picking of P and S arrivals for the youngest event in the family to ensure
 219 consistent phase pick quality for the later analysis.

220 **2.2 Repeating earthquakes detection**

221 The core of our detection criterion is a threshold based on the cross-correlation
 222 of different events recorded at different stations. We assessed the sensitivity of the re-
 223 peating earthquake catalog to variations in the length of the cross-correlation window,
 224 waveform filtering parameters, and the specific correlation threshold employed. We
 225 also compared our cross-correlation-derived catalog with one constructed using coher-
 226 ence as a measure of similarity (as used by some studies, e.g. Materna et al. (2018)).
 227 We chose not to use coherence as our detection metric because it introduced additional
 228 parameters, namely the frequency band over which coherence was assessed, without
 229 significantly changing our results.

230 A cross-correlation window-length of 40 s, encompassing both P- and S-arrivals,
 231 has commonly been used in studies elsewhere to detect repeating earthquakes (Uchida
 232 et al., 2003, 2004; Yamashita et al., 2012). However, because the event-to-station
 233 path-length in our study area varies between <10 km and ~180 km, S-P times and
 234 coda durations also varied strongly between different events and different stations.
 235 We therefore chose to use a waveform length dependent on coda-duration to compute
 236 robust cross-correlations that captured similar amounts of signal for different event-
 237 station paths. We found that using 75% of the coda duration (defined herein as when
 238 the signal to noise ratio first dropped below unity) was appropriate for calculating the
 239 normalized cross-correlation, as it includes both P- and S-arrivals and most of the coda
 240 and resulted in the maximum normalized cross-correlation for visibly similar events.
 241 When the cross-correlation window length was less than 50% or greater than 100% of
 242 the coda length, the resulting cross-correlation between earthquakes in the prospective
 243 families was found to be distinctly lower. If we could not identify the end of the coda,
 244 due to the level of noise in the waveform, a window-length of 25 s was imposed. In all
 245 cases, our cross-correlation windows started 1 s before the identified P-arrival. Cross-
 246 correlations were computed after aligning the waveforms on the P-arrivals, with each
 247 waveform allowed to shift by as much as 1 s in order to achieve optimal alignment and
 248 thereby allow the maximum cross-correlation to be calculated.

249 Prior to computing cross-correlations, we detrended the data and applied a
 250 fourth-order bandpass filter between 1 and 20 Hz. The lowcut of this filter was chosen
 251 to remove low-frequency noise found to dominate the signal at some of the broad-
 252 band stations. We tested the response of the calculated normalised cross-correlation
 253 to changes in the highcut parameter but observed no strong variations and opted for
 254 a 20 Hz highcut as this retains a wide range of frequencies while ameliorating high-
 255 frequency noise.

256 Finally, to test the sensitivity of our catalog to changes in cross-correlation thresh-
 257 old, we determined which earthquakes would be retained as the correlation threshold
 258 was increased from 0.90 to 0.99 at intervals of 0.01. We required this threshold to be
 259 exceeded on at least two stations. We found that the number of families that were
 260 rejected as repeating and the number of events in each family varied more when the
 261 threshold was set to less than 0.95, compared to when it was larger than 0.95. When
 262 the threshold was set to greater than 0.95, families were rejected due to small differ-
 263 ences in the background noise of the waveform rather than significant differences in the
 264 signal. We therefore chose to use a threshold of 0.95, as used in multiple other repeat-
 265 ing earthquake studies (e.g. Uchida & Bürgmann, 2019, and references therein). We
 266 were unable to require high cross-correlation on more than two stations due to station

continuity: nearby stations generally provide the highest cross-correlation values due to higher signal-to-noise ratios, but prior to 2003 there only two permanent broadband seismometers and seven permanent short period seismometers within 120 km of the main clusters of repeating earthquakes. This station continuity limits our analysis to times after 2003.

2.3 Location procedure

We undertook absolute location and relative relocation of all possible repeating earthquakes to verify that events identified with the correlation-based detection criterion are indeed closely spaced. The phase picks in the original GeoNet catalog vary in quality, having been made using both automatic and manual methods, so we conducted additional phase picking for all events in our repeating earthquake catalog to ensure consistency. We manually picked P- and S-wave first arrivals for the youngest event in each family, which is commonly the best-recorded event due to the general increase with time of the number of stations, and identified P-wave polarities for later focal mechanism analysis. This yielded a total of 1,159 P-picks and 939 S-picks for the 133 possible families, resulting in an average of 9 P-picks and 7 S-picks for each of the youngest events. Fewer S-picks than P-picks were made due to the P-coda obscuring the S-arrival at short epicentral distances. Since all events in a particular family are, by definition, well-correlated we were able to compute accurate (sub-sample) relative pick times for all the other events using the EQcorrscan cross-correlation pick correction function `xcorr_pick_family()` (Chamberlain et al., 2018). This function follows the approach of Deichmann and Garcia-Fernandez (1992) and computes a moving window cross-correlation that is represented at each epoch by a parabolic function fit to the five samples around the maximum correlation. The peak of this parabola is taken as the time-shift of the pick. This workflow not only provides accurate and consistent phase arrivals but also provides 572 additional phase picks compared to the GeoNet catalog from which we started.

All the events in our catalog have hypocenters computed by GeoNet but the location algorithms and velocity models with which they have been determined have changed throughout the catalog period. To generate consistent locations, and to take advantage of our additional phase-picks, we computed absolute locations for all events using the NonLinLoc location software (Lomax et al., 2000) and the New Zealand-wide 3D velocity model (version 2.1) (Eberhart-Phillips et al., 2017; Eberhart-Phillips & Bannister, 2015). We also computed absolute locations using the SIMUL2014 software (Eberhart-Phillips et al., 2015), but found that this gave poorer fits to our picks compared to the NonLinLoc locations.

To test whether the earthquakes we identified as repeating based on correlation criteria truly overlap in source area, we also undertook relative relocation of all events. Due to the number and positions of seismometers in the network changing and generally improving with time, the absolute locations of older earthquakes are generally of poorer quality than the more recent earthquakes. To cope with this variable quality, and to test whether earthquakes within each family overlap, we used the absolute location of the youngest event in each family as the starting location for the relocation of all other events within the family. Using this starting location allows us to verify whether the earthquakes within a family can be well-fit by overlapping locations, rather than necessarily providing highly accurate relative locations between families. For this relocation we used the GrowClust software of Trugman and Shearer (2017) with the onshore 1D velocity model from Yarce et al. (2019).

315

2.4 Focal Mechanisms

316

317

318

319

320

We constructed focal mechanisms for the youngest event in each family, using the manually picked P-wave first-motion polarities in the FPFIT (Reasenberg, 1985) routine implemented in SEISAN (Havskov & Ottemoller, 1999). The event locations were fixed to the locations obtained using GrowClust, no relative weightings were applied to the polarities and a 2° increment was used to search for the best fit solution.

321

2.5 Magnitudes

322

323

324

325

326

327

328

329

330

331

332

333

334

335

Alongside variations in location procedure throughout the cataloged period, the magnitudes procedures used by GeoNet have also varied. To generate consistent magnitudes we recomputed the local magnitudes of the youngest event in each family, and computed relative magnitudes for all other events within a family. To compute the magnitudes of the youngest events in each family we first generated automatic amplitude picks for the horizontal components of each station picked. Automatic amplitude picks were made on data that were filtered between 1 and 20 Hz, then instrument corrected and convolved with the response of a Wood Anderson seismometer. The response of the pre-filter was subsequently corrected for in the resulting amplitude picks. The resulting amplitude picks were used to compute a consistent set of station correction and attenuation terms based on the GeoNet-computed local magnitudes for these events. The magnitudes for all other events within families were computed using a correlation-weighted average of the relative-amplitudes, following the method of Schaff and Richards (2014).

336

3 Results

337

338

339

340

341

342

343

344

345

We identified 62 repeating earthquake families active between 2003 and 2018, which collectively contained 160 individual earthquakes. The 62 families are clustered into more active regions around the Raukumara Peninsula (Figure 2). To facilitate further description, we assigned each family to one of eleven regional groups, which were named based on their proximity to local population centers (see Figure 2). Within each of the regional groups, families were assigned a two letter geographic code and a two-digit number, based on the relative order of the first recorded repeating event in the family. The number of families within each of the regional groups ranges from one to 34 (Figure 2 and Table 1).

346

347

348

349

350

351

352

353

354

355

The repeating earthquake families identified have a magnitude range of M_L 0.6 to M_L 5.3, and the recurrence intervals range between <1 yr and ~ 12 yrs (Table 1). The number of repeating events in each of the families ranges from two to five, with only five families containing more than three events. In Figure 3, the waveforms of the repeating events in four region groups are depicted, highlighting the visual similarities between the events in each of the families. In Figure 3, WA01 is the largest magnitude family in the catalog and is the only family located to the northwest of the Raukumara Peninsula, TA01 is the furthest offshore family (~ 30 km), TS01 locates ~ 10 km offshore just south of Tolaga Bay and NU01 and NU02 locate onshore to the west of the Māhia Peninsula.

356

357

358

359

360

361

362

Focal mechanism for 56 of the 62 families were constructed, with the remaining six families not having focal mechanism created due to a lack to first arrival polarities being identified during manual picking. The focal mechanisms of the repeating earthquake families are consistent with both upper and lower intra-plate faulting, as well as faulting along the subduction interface. Due to the location of the families with respect to the GeoNet seismic network, many of the focal mechanisms are poorly constrained, with maximum one sigma errors for the strike, dip and rake being 34.0° , 30.0° and 54.0°

363 respectively. The average one sigma error in the strike, dip and rake of the focal
 364 mechanisms are 7.06° , 8.67° and 14.53° respectively.

365 The repeating earthquake catalog we have constructed is intrinsically no-more
 366 complete than the GeoNet catalog. However, the magnitude of completeness of the
 367 GeoNet catalog around the Raukumara region varied from $\sim M3$ in 2003 to $\sim M2$
 368 in 2019 (Figure 4 a). In the Raukumara repeating earthquake catalog, only nine of
 369 the 160 identified repeating earthquakes have calculated local magnitudes which are
 370 less than $M_L 2$ (Figure 4 b). As the catalog was formed using the GeoNet catalog, if
 371 smaller magnitude events were not identified in the GeoNet catalog, then they would
 372 not be included in this repeating earthquake catalog.

373 4 Discussion

374 4.1 Spatial and temporal relationships to other subduction phenomena

375 Based on the location of the youngest event and focal mechanism of each family,
 376 we categorized the repeating earthquakes as occurring on the subduction interface,
 377 within the Australian plate, or within the Pacific plate. Families which had a low-
 378 angle reverse focal mechanism and were within ~ 5 km of the C. A. Williams et al.
 379 (2013) interface model were assumed to be occurring on the interface, or associated
 380 faults, and the remaining families were assigned to the over-riding or down-going plate
 381 based on their location relative to those events. As a result, 40 families are concluded
 382 to occur within the over-riding Australian Plate, exhibiting a range of faulting types,
 383 15 occur along the subduction interface, and 7 are in the down-going Pacific Plate and
 384 exhibit predominantly strike-slip and normal faulting focal mechanisms. However, 35
 385 of the families not concluded to occur on the plate interface, due to the type of faulting
 386 are located within ± 5 km of the interface (Figure 5). While the focal mechanism of
 387 WA01 is consistent with interface faulting, the mean depth (58 km) of the family is
 388 slightly shallower than the interface model, so is not consistent with being on the
 389 interface.

390 All of the repeating earthquake families inferred, on the basis of their hypocenters
 391 and focal mechanisms, to occur on the subduction interface lie within regions identified
 392 by (Wallace et al., 2012) to have low-coupling (Figure 5). The spatial relationship of
 393 the intraplate families to interface locking is less clear, with only the Pouawa and
 394 Tolaga-South families located above, and below, the locked-sliding transition.

395 Heise et al. (2017) recently investigated the relationship between geodetically
 396 observed locking of the subduction interface (Wallace et al., 2012; Dimitrova et al.,
 397 2016) and the physical properties of the interface inferred from electrical resistivity
 398 observations. They argued that areas in which the interface is locked and the upper
 399 plate is undergoing areal contraction are electrically resistive, notably between the
 400 Māhia Peninsula and Tolaga Bay, and concluded that the frictional coupling of the
 401 interface is governed by low fluid or sediment volumes.

402 We observe that repeating earthquake families occurring on the subduction in-
 403 terface and in the over-riding plate in the Te Karaka group coincide with an area of
 404 distinctively high resistivity on and above the interface (200–600 Ω m) identified by
 405 Heise et al. (2017); the single family in Whatatutu group, which occurs in the Pacific
 406 plate, lies beneath this zone of high resistivity. However, repeating earthquakes occur-
 407 ring on the interface or in the upper plate in the the Māhia and Nūhaka groups in the
 408 south of the Peninsula and the Tolaga Bay and Tokamaru Bay groups further north
 409 occur within zones of relatively low interface resistivity (≤ 20 Ω m; cf. Figure 2 of Heise
 410 et al., 2017). Moreover, no clear spatial relationship is evident between the epicenters
 411 of repeating earthquakes and areal strain rates (Figure 4 of Dimitrova et al., 2016).

Active-source seismic imaging has revealed two seamounts subducting offshore between the Māhia Peninsula and Tokomaru Bay (Figure 5, after Bell et al., 2010). Additionally, high-amplitude reflections have been observed adjacent to the plate interface, down-dip of the subducting seamounts (Bell et al., 2010). Bell et al. (2010) interpreted these high-amplitude reflections as fluid-rich sediments, entrained by the subducting seamount. The Pouawa group families (offshore to the southeast of Tolaga Bay) are located down-dip of the southern seamount, coincident with the high-amplitude reflectors mapped by Bell et al. (2010) and down-dip of the “burst-type” repeating earthquakes identified by Shaddox and Schwartz (2019), but no repeating earthquakes have been detected in the vicinity of the northern seamount.

When the location of the repeating earthquakes are compared to the location of previously identified slow slip, the Te Karaka, Whatatutu, Tokomaru-Tolaga and Te Puia groups locate along the down-dip periphery of the identified cumulative slow-slip patch (Figure 2; Wallace & Beavan, 2010; Wallace et al., 2016; Koulali et al., 2017). In comparison, the Nūhaka and Māhia repeating earthquakes transect the southern extent of the modeled slow-slip patch (Wallace & Beavan, 2010; Wallace et al., 2016). Furthermore, the Pouawa and Tolaga-South group families lie along the boundary between two persistent patches of slow-slip which occur to the northeast and southwest of the families locations (Wallace & Beavan, 2010; Wallace et al., 2016).

We next consider the temporal relationships between the repeating earthquakes and previously described slow slip. Such relationships have been extensively documented throughout the Japan subduction zone (Gardonio et al., 2018; Kato et al., 2012; Igarashi et al., 2003; Uchida et al., 2004, 2006; Uchida & Matsuzawa, 2013; Uchida et al., 2016) and we similarly compare the timing of individual repeating earthquakes and their cumulative moment release to time-series of geodetically measured displacement and recognized episodes of slow slip (Figure 6). For the purposes of comparison with measured deformation, we focus on the displacement time-series from GeoNet’s global navigation satellite system station near Gisborne (“GISB”) as it provides a general reference for motion in the region of interest and has been operating continuously since 2002. We compute the moment of each repeating earthquake by converting the calculated local magnitudes using the following scaling relationship in Aki (1972).

$$\log(M_0) = 1.4 \log(M_L) + 17.0 \quad (1)$$

We observe some episodes of slow slip to be accompanied by repeating earthquake activity in some families, such as in 2004 (TA and TP groups) and in 2011 (TA and TP groups again) (Figure 6). However, this is not consistent for all slow-slip events or regional repeating earthquake groups. Of the 31 slow-slip events previously identified to the north of Māhia Peninsula, five are not clearly associated with a step in the cumulative moment curve of any repeating earthquake groups. The Ruatōria and Pouawa Groups show the clearest correlation between the occurrence of the repeating earthquakes and the occurrence of a slow-slip event (Figure 6, e and f respectively). For the Ruatōria Group, four of the seven repeating earthquakes occur during the approximate timing of the slow-slip events that occurred after 2008, with the slow-slip events occurring from the Māhia Peninsula to Puketiti (Figure 6e). These earthquakes account for ~45% of the total moment of the group. Moreover, six events in the Pouawa Group correspond to the occurrence of slow-slip events, with four of these slow-slip events occurring around Gisborne.

Overall, the repeating earthquakes show little consistent response to any of the three large earthquakes that have occurred in the time spanned by this study. However, the 2008 Gisborne earthquake was followed 10 days later by a repeating earthquake in the Pouawa group (Figure 6f), and the 2016 Kaikōura earthquake was similarly followed, 19 days later, by the next event in that same family. Similarly, both the Te

463 Araroa and Kaikōura earthquakes were followed within days by repeating earthquakes
464 in the Tokomaru-Tolaga area (Figure 6i).

465 Distinguishing the repeating earthquakes on the basis of tectonic position (Fig-
466 ure 6m) reveals marked steps in the cumulative moment release of earthquakes oc-
467 curring on the subduction interface at the time of slow slip in early 2010. The early
468 2010 episode of slow slip occurred between Tolaga Bay and Māhia (Wallace & Beavan,
469 2010). The two largest increments of moment release associated with Pacific Plate re-
470 peating earthquakes occurred in late 2005 and early 2011 and neither is associated with
471 recognized slow slip. Australian Plate repeating earthquakes exhibit a generally con-
472 stant rate of moment release with the largest increments showing no clear relationship
473 to episodes of slow slip.

474 Jacobs et al. (2016) analyzed seismicity associated with slow-slip events along
475 the length of the Hikurangi Subduction Margin and found that three of the largest
476 sequences occurred in 2007, 2009 and 2010 approximately 20 km to the east of the
477 Raukumara Peninsula. We observe increases in the number of repeating earthquakes
478 occurring in the Australian Plate at the times of both the 2009 and 2010 sequences but
479 not the 2007 sequence. Similar patterns are observed with the Pacific Plate families,
480 with the rate of repeating earthquakes increasing in response to the 2010 sequence
481 but not the 2007 or 2009 sequences. However, no response to any of these sequences
482 is observed for the repeating earthquakes inferred to occur on the subduction inter-
483 face. The patterns we have observed are consistent with the findings of Delahaye et al.
484 (2009), who identified microearthquakes occurring either on the subduction interface
485 or just below that were triggered down-dip of a slow-slip event in October–November
486 2004. The repeating earthquakes families also occur in similar locations to the micro-
487 seismicity identified by Yarce et al. (2019), with only one repeating earthquake family
488 (TS01) occurring in a seismicity gap identified in that study. Moreover, work done
489 by Bassett et al. (2014), to try and explain the occurrence of slow-slip in the region,
490 identified slower wavespeeds and the possibility of near-lithostatic fluid pressures on
491 the interface, which may also have an effect on the repeating earthquakes, alongside
492 inferred fluid-pressure cycling related to SSE occurrence (Warren-Smith et al., 2019).

493 We also compared the timing of three large earthquakes to the timing of the
494 occurrence of repeating earthquakes. Two of these earthquakes occurred within the
495 area of interest around the Raukumara Peninsula. The first was the M_W 6.6 Gisborne
496 earthquake, which occurred on the 20th of December 2007 UTC, 64 km from Gisborne
497 at a depth of 40 km, in the subducting Pacific Plate (Francois-Holden et al., 2008).
498 The second was the M_W 7.1 Te Araroa earthquake 1st of September 2016 UTC, at
499 a depth of 19 km, also in the subducting Pacific Plate (Warren-Smith et al., 2018).
500 The timing of the 2016 M_W 7.8 Kaikōura earthquake was also compared to the timing
501 of repeating earthquakes despite not occurring within the study area. This is due to
502 the Kaikōura earthquake triggering slow-slip in the study region following the earth-
503 quake (Wallace et al., 2018). We observe a step in the cumulative moment in three of
504 the regional groups following the three large earthquakes previously mentioned. The
505 Pouawa Group is the only regional group where steps in the cumulative moment is
506 observed following to the Gisborne M_W 6.6 earthquake, occurring five months follow-
507 ing the event, as well as a step 19 days after the Kaikōura earthquake (Figure 6f).
508 Three days following Kaikōura earthquake, a step in the Tokomaru-Tolaga Group is
509 also observed (Figure 6i). Moreover, the Te Puia Group is the only regional group
510 which showed a step in the cumulative moment following the Te Araroa earthquake
511 (Figure 6f). We see no evidence for direct triggering of repeating earthquakes following
512 these large earthquakes.

513 4.2 Scaling relationships for the the Raukumara Peninsula repeating earth- 514 quakes

515 Nadeau and Johnson (1998) proposed that the magnitudes of repeating earth-
516 quakes should scale as a function of recurrence interval, based on the cyclic loading and
517 stress release model. They demonstrated this to be the case near Parkfield, California,
518 obtaining the relationship

$$\log(T) = 4.85 + 0.17 \log(M_O) \quad (2)$$

519 where T is the recurrence interval in seconds and M_O is the seismic moment in dyne-
520 cm. This scaling of moment with recurrence interval has since been examined and
521 verified in other many other locations (K. H. Chen et al., 2007; T. Chen & Lapusta,
522 2009; Dominguez et al., 2016; Johnson, 2010; Lengliné & Marsan, 2009; Marone et al.,
523 1995; Mavrommatis et al., 2015; Mesimeri & Karakostas, 2018; Nadeau & Johnson,
524 1998; Peng et al., 2005; Schaff & Richards, 2011; Uchida, 2019; Yu, 2013). Slight
525 variations in the relationship have been observed between different regions, as have
526 changes in scaling before and after nearby large earthquakes (Schaff & Richards, 2011;
527 Yu, 2013; Chaves et al., 2020).

528 To investigate this relationship in the New Zealand context, we used the average
529 recurrence interval for each of the repeating earthquake families and the moment of
530 the youngest event in the family (Figure 7). The magnitude of the youngest event
531 was taken to represent each family as a whole, rather than averaging the values of all
532 the events in a family, for two reasons: first, the magnitudes of each of the families
533 were extremely similar; and second, it was assumed that the youngest event in each
534 family had the best-constrained magnitude and lowest associated error due to overall
535 improvements in network coverage and geometry.

536 In Figure 7, families with durations shorter than six months were removed be-
537 fore the relationships were calculated, as the relationship identified by Nadeau and
538 Johnson (1998) was for long duration repeating earthquake families, and we wanted
539 to compare similar families. Furthermore, these short duration families masked any
540 identifiable relationship between recurrence interval and seismic moment. As can be
541 seen in Figure 7, the relationship between seismic moment and recurrence interval for
542 the Raukumara Peninsula repeating earthquake families is weaker than the relation-
543 ship identified by Nadeau and Johnson (1998). However, the 95% confidence intervals
544 for both the gradient and the intercept include the values for the Parkfield repeating
545 earthquakes. Due to the scatter in the data for all the plate locations, the confidence
546 intervals are extremely wide, and prevent us from determining a reliable relationship.
547 Overall, while we found that the Raukumara Peninsula repeating earthquake families'
548 relationship between recurrence interval and seismic moment followed a very weakly
549 positive trend, consistent with the findings of repeating earthquake studies elsewhere,
550 the uncertainty associated with these trends is very large. This places uncertainty on
551 applying other relationships established by Nadeau and Johnson (1998) to the Rauku-
552 mara Peninsula repeating earthquakes. We speculate that the scatter we observe may
553 be due to the influence of variable slip-rates associated with nearby slow-slip episodes.

554 4.2.1 Calculating the slip-rate of the repeating earthquake families

555 Using 53 repeating earthquake families, from the Parkfield segment of the San
556 Andreas fault, and 8 repeating earthquake families from the Stone Canyon section,
557 Nadeau and Johnson (1998) derived a formula which relates the average seismic mo-
558 ment to the average amount of slip of a repeating earthquake family (Equation 3).
559 The Parkfield segment families had a magnitude range of $M_W -0.7-1.4$, while the
560 Stone Canyon families were added to the analysis to extend the magnitude range to

561 M_W 3.7–6.0. Nadeau and Johnson (1998) derived the relationship:

$$\log(d) = -2.36 + 0.17 \log(M_O) \quad (3)$$

562 where d is the average amount of slip for a repeating earthquake family in cm, and
 563 M_0 is the average seismic moment of the repeating earthquake family, in dyne-cm.
 564 This relationship has also been applied to other tectonic setting and studies, including
 565 Japan, to determine the slip of identified repeating earthquake families (Uchida et al.,
 566 2003). Based on the magnitude range the relationship was derived over, and that it
 567 has been universally applied to different settings, we applied the relationship to the
 568 Raukumara Peninsula repeating earthquake families, to calculate the slip-rate.

569 Preliminary slip-rates calculated for the Raukumara Peninsula repeating earth-
 570 quake families range from < 10 mm/yr up to ~ 80 mm/yr, when the families with ex-
 571 tremely short family durations (less than 1 year) are excluded. Generally, the shorter
 572 the family duration the faster the slip-rate will be. This trend follows previously es-
 573 tablished relationships for Parkfield and Japan, with short duration families having
 574 slip-rates which are significantly higher than the tectonic loading rate, compared to
 575 long-duration families. TT19 is the only interface family that has a calculated slip-
 576 rate close to the plate convergence rate (31 mm/yr compared to 45 mm/yr). However,
 577 due to the differences observed in the seismic moment–recurrence interval relationship
 578 previously mentioned, applying the Parkfield repeating earthquake slip model to the
 579 Raukumara Peninsula families, may not be appropriate.

580 We close this section by noting that in this first New Zealand study of earthquakes
 581 we made no attempt to detect events not otherwise listed in the original GeoNet
 582 catalog. Future work using matched-filter methods to detect lower-magnitude events
 583 is likely to greatly expand the number of repeating earthquakes detected, and provide
 584 a more robust basis for investigating scaling relationships and the use of repeating
 585 earthquakes to quantify slip rates.

586 5 Conclusions

587 We have identified 62 repeating earthquake families containing a total of 160
 588 earthquakes that occurred between 2003 and 2018 in the vicinity of the Raukumara
 589 Peninsula, on the northern Hikurangi Subduction Margin. These families represent a
 590 range of faulting types and occur along the subduction interface and in the overlying
 591 and subducting plates. We observe steps in the cumulative moment of the repeating
 592 earthquakes coinciding with 26 of 31 previously identified slow-slip events. We also
 593 compared the Raukumara Peninsula families to families and repeating earthquake
 594 relationships previously identified around Parkfield, California. When comparing re-
 595 currence interval–seismic moment relationships, we identified a similar trend between
 596 the two locations, and when calculating the slip-rate of the families, only one was
 597 found to have an estimated slip-rate that matched the plate convergence rate.

598 Acknowledgments

599 We gratefully acknowledge funding provided by the Marsden Fund of the Royal Society
 600 Te Apārangi (project 17-VUW-121) and the Earthquake Commission Programme in
 601 Seismology and Tectonic Geodesy at Victoria University of Wellington–Te Herenga
 602 Waka. We also acknowledge the New Zealand GeoNet project and its sponsors EQC,
 603 GNS Science and LINZ, for providing the data used in this study. The figures in
 604 this paper were constructed using the Generic Mapping Tools (Wessel et al., 2019),
 605 matplotlib (Hunter, 2007), and ObsPy (Beyreuther et al., 2010). We acknowledge
 606 GNS Science for maintaining and providing access to the New Zealand Active Faults
 607 Database through the website data.gns.cri.nz/af/ (last accessed 3 December 2020).

References

- 608
- 609 Abercrombie, Rachel E. and Chen, Xiaowei and Zhang, Jiewen. (2020). Repeat-
 610 ing Earthquakes with Remarkably Repeatable Ruptures on the San Andreas
 611 Fault at Parkfield. *Geophysical Research Letters*, e2020GL089820. doi:
 612 <https://doi.org/10.1029/2020GL089820>
- 613 Aki, K. (1972). Scaling law of earthquake source time-function. *Geophysical Journal*
 614 *International*, 31(1-3), 3–25.
- 615 Barnes, P. M., Lamarche, G., Bialas, J., Henrys, S., Pecher, I., Netzeband, G. L.,
 616 ... Crutchley, G. (2010). Tectonic and geological framework for gas hydrates
 617 and cold seeps on the Hikurangi subduction margin, New Zealand. *Marine*
 618 *Geology*, 272(1-4), 26–48.
- 619 Bassett, D., Sutherland, R., & Henrys, S. (2014). Slow wavespeeds and fluid over-
 620 pressure in a region of shallow geodetic locking and slow slip, Hikurangi sub-
 621 duction margin, New Zealand. *Earth and Planetary Science Letters*, 389,
 622 1–13.
- 623 Beanland, S. (1995). *The North Island Dextral Fault Belt, Hikurangi Subduction*
 624 *Margin, New Zealand: A Thesis Submitted for the Degree of Doctor of Philos-*
 625 *ophy [in Geology], Victoria University of Wellington.* Victoria University of
 626 Wellington.
- 627 Bell, R., Holden, C., Power, W., Wang, X., & Downes, G. (2014). Hikurangi mar-
 628 gin tsunami earthquake generated by slow seismic rupture over a subducted
 629 seamount. *Earth and Planetary Science Letters*, 397, 1–9.
- 630 Bell, R., Sutherland, R., Barker, D. H. N., Henrys, S., Bannister, S., Wallace, L., &
 631 Beavan, J. (2010). Seismic reflection character of the Hikurangi subduction
 632 interface, New Zealand, in the region of repeated Gisborne slow slip events.
 633 *Geophysical Journal International*, 180(1), 34–48.
- 634 Beyreuther, M., Barsch, R., Krischer, L., Megies, T., Behr, Y., & Wassermann, J.
 635 (2010). ObsPy: A Python toolbox for seismology. *Seismological Research*
 636 *Letters*, 81(3), 530–533.
- 637 Bohnhoff, M., Wollin, C., Domigall, D., Küperkoch, L., Martínez-Garzón, P.,
 638 Kwiątek, G., ... Malin, P. E. (2017). Repeating Marmara Sea earthquakes:
 639 indication for fault creep. *Geophysical Journal International*, 210(1), 332–339.
- 640 Chamberlain, C. J., Hopp, C. J., Boese, C. M., Warren-Smith, E., Chambers, D.,
 641 Chu, S. X., ... Townend, J. (2018). EQcorrscan: Repeating and near-
 642 repeating earthquake detection and analysis in Python. *Seismological Research*
 643 *Letters*, 89(1), 173–181.
- 644 Chaves, E. J., Schwartz, S. Y., & Abercrombie, R. E. (2020). Repeating earthquakes
 645 record fault weakening and healing in areas of megathrust postseismic slip.
 646 *Science Advances*, 6(32). doi: 10.1126/sciadv.aaz9317
- 647 Chen, K. H., Bürgmann, R., & Nadeau, R. M. (2013). Do earthquakes talk to each
 648 other? Triggering and interaction of repeating sequences at Parkfield. *Journal*
 649 *of Geophysical Research: Solid Earth*, 118(1), 165–182.
- 650 Chen, K. H., Bürgmann, R., Nadeau, R. M., Chen, T., & Lapusta, N. (2010).
 651 Postseismic variations in seismic moment and recurrence interval of repeating
 652 earthquakes. *Earth and Planetary Science Letters*, 299(1-2), 118–125.
- 653 Chen, K. H., Nadeau, R. M., & Rau, R. (2007). Towards a universal rule on the re-
 654 currence interval scaling of repeating earthquakes? *Geophysical Research Let-*
 655 *ters*, 34(16), 1–5.
- 656 Chen, K. H., Nadeau, R. M., & Rau, R.-J. (2008). Characteristic repeating earth-
 657 quakes in an arc-continent collision boundary zone: The Chihshang fault of
 658 eastern Taiwan. *Earth and Planetary Science Letters*, 276(3-4), 262–272.
- 659 Chen, T., & Lapusta, N. (2009). Scaling of small repeating earthquakes explained by
 660 interaction of seismic and aseismic slip in a rate and state fault model. *Journal*
 661 *of Geophysical Research: Solid Earth*, 114(B1), 1–12.

- 662 Clark, K., Howarth, J., Litchfield, N., Cochran, U., Turnbull, J., Dowling, L., ...
 663 Wolfe, F. (2019). Geological evidence for past large earthquakes and tsunamis
 664 along the Hikurangi subduction margin, New Zealand. *Marine Geology*.
- 665 Deichmann, N., & Garcia-Fernandez, M. (1992). Rupture geometry from high-
 666 precision relative hypocentre locations of microearthquake clusters. *Geophysical
 667 Journal International*, 110(3), 501–517.
- 668 Delahaye, E. J., Townend, J., Reyners, M. E., & Rogers, G. (2009). Microseismicity
 669 but no tremor accompanying slow slip in the Hikurangi subduction zone, New
 670 Zealand. *Earth and Planetary Science Letters*, 277(1-2), 21–28.
- 671 Dimitrova, L. L., Wallace, L. M., Haines, A. J., & Williams, C. A. (2016). High-
 672 resolution view of active tectonic deformation along the Hikurangi subduction
 673 margin and the Taupo Volcanic Zone, New Zealand. *New Zealand Journal of
 674 Geology and Geophysics*, 59(1), 43–57.
- 675 Dominguez, L. A., Taira, T., & Santoyo, M. A. (2016). Spatiotemporal variations
 676 of characteristic repeating earthquake sequences along the Middle America
 677 Trench in Mexico. *Journal of Geophysical Research: Solid Earth*, 121(12),
 678 8855–8870.
- 679 Doser, D. I., & Webb, T. H. (2003). Source parameters of large historical
 680 (1917–1961) earthquakes, North Island, New Zealand. *Geophysical Journal
 681 International*, 152(3), 795–832.
- 682 Douglas, A., Beavan, J., Wallace, L., & Townend, J. (2005). Slow slip on the north-
 683 ern Hikurangi subduction interface, New Zealand. *Geophysical Research Let-
 684 ters*, 32(16), 1–4.
- 685 Eberhart-Phillips, D., & Bannister, S. (2015). 3-D imaging of the northern Hiku-
 686 rangi subduction zone, New Zealand: variations in subducted sediment, slab
 687 fluids and slow slip. *Geophysical Journal International*, 201(2), 838–855.
- 688 Eberhart-Phillips, D., Bannister, S., & Reyners, M. (2017). New Zealand Wide
 689 model 2.1 seismic velocity model for New Zealand. *Zenodo*. Retrieved from
 690 <https://doi.org/10.5281/zenodo.1043558> doi: 10.5281/zenodo.1043558
- 691 Eberhart-Phillips, D., Reyners, M., & Bannister, S. (2015). A 3D QP attenuation
 692 model for all of New Zealand. *Seismological Research Letters*, 86(6), 1655–
 693 1663.
- 694 Francois-Holden, C., Bannister, S., Beavan, J., Cousins, J., Field, B., McCaffrey, R.,
 695 ... Samsonov, S. (2008). The Mw 6.6 Gisborne earthquake of 2007: Prelimi-
 696 nary records and general source characterisation. *Bulletin of the New Zealand
 697 Society for Earthquake Engineering*, 41(4), 266–277.
- 698 Gardonio, B., Marsan, D., Socquet, A., Bouchon, M., Jara, J., Sun, Q., ...
 699 Campillo, M. (2018). Revisiting slow slip events occurrence in Boso Penin-
 700 sula, Japan, combining GPS data and repeating earthquakes analysis. *Journal
 701 of Geophysical Research: Solid Earth*, 123(2), 1502–1515.
- 702 Hatakeyama, N., Uchida, N., Matsuzawa, T., & Nakamura, W. (2017). Emergence
 703 and disappearance of interplate repeating earthquakes following the 2011 M9.0
 704 Tohoku-oki earthquake: Slip behavior transition between seismic and aseismic
 705 depending on the loading rate. *Journal of Geophysical Research: Solid Earth*,
 706 122(7), 5160–5180.
- 707 Havskov, J., & Ottemoller, L. (1999). SEISAN earthquake analysis software. *Seis-
 708 mological Research Letters*, 70(5), 532–534.
- 709 Heise, W., Caldwell, T. G., Bannister, S., Bertrand, E. A., Ogawa, Y., Bennie, S. L.,
 710 & Ichihara, H. (2017). Mapping subduction interface coupling using magne-
 711 totellurics: Hikurangi margin, New Zealand. *Geophysical Research Letters*,
 712 44(18), 9261–9266.
- 713 Hunter, J. D. (2007). Matplotlib: A 2D graphics environment. *Computing in science
 714 & engineering*, 9(3), 90–95.
- 715 Igarashi, T., Matsuzawa, T., & Hasegawa, A. (2003). Repeating earthquakes and
 716 interplate aseismic slip in the northeastern Japan subduction zone. *Journal of*

- 717 *Geophysical Research: Solid Earth*, 108(B5), 1–8.
- 718 Jacobs, K. M., Savage, M. K., & Smith, E. C. G. (2016). Quantifying seismicity
719 associated with slow slip events in the Hikurangi margin, New Zealand. *New*
720 *Zealand Journal of Geology and Geophysics*, 59(1), 58–69.
- 721 Johnson, L. R. (2010). An earthquake model with interacting asperities. *Geophysical*
722 *Journal International*, 182(3), 1339–1373.
- 723 Kato, A., Obara, K., Igarashi, T., Tsuruoka, H., Nakagawa, S., & Hirata, N. (2012).
724 Propagation of slow slip leading up to the 2011 Mw 9.0 Tohoku-Oki earth-
725 quake. *Science*, 335(6069), 705–708.
- 726 Koulali, A., McClusky, S., Wallace, L., Allgeyer, S., Tregoning, P., D’Anastasio,
727 E., & Benavente, R. (2017). Slow slip events and the 2016 Te Araroa Mw
728 7.1 earthquake interaction: Northern Hikurangi subduction, New Zealand.
729 *Geophysical Research Letters*, 44(16), 8336–8344.
- 730 Krischer, L., Megies, T., Barsch, R., Beyreuther, M., Lecocq, T., Caudron, C., &
731 Wassermann, J. (2015). ObsPy: A bridge for seismology into the scientific
732 Python ecosystem. *Computational Science & Discovery*, 8(1), 14003.
- 733 Langridge, R., Ries, W., Litchfield, N., Villamor, P., Van Dissen, R., Barrell, D., ...
734 others (2016). The new zealand active faults database. *New Zealand Journal*
735 *of Geology and Geophysics*, 59(1), 86–96.
- 736 Lengliné, O., & Marsan, D. (2009). Inferring the coseismic and postseismic stress
737 changes caused by the 2004 Mw6 Parkfield earthquake from variations of re-
738 currence times of microearthquakes. *Journal of Geophysical Research: Solid*
739 *Earth*, 114(B10), 1–19.
- 740 Li, C., Peng, Z., Yao, D., Guo, H., Zhan, Z., & Zhang, H. (2018). Abundant af-
741 tershock sequence of the 2015 Mw7. 5 Hindu Kush intermediate-depth earth-
742 quake. *Geophysical Journal International*, 213(2), 1121–1134.
- 743 Litchfield, N. J., Clark, K. J., Cochran, U. A., Palmer, A. S., Mountjoy, J., Mueller,
744 C., ... Villamor, P. (2020, 1). Marine Terraces Reveal Complex Near-Shore
745 Upper-Plate Faulting in the Northern Hikurangi Margin, New Zealand. *Bul-*
746 *letin of the Seismological Society of America*, XX, 1–25. Retrieved from
747 <https://doi.org/10.1785/0120190208> doi: 10.1785/0120190208
- 748 Lomax, A., Virieux, J., Volant, P., & Berge-Thierry, C. (2000). Probabilistic earth-
749 quake location in 3D and layered models. In *Advances in seismic event location*
750 (pp. 101–134). Springer.
- 751 Lui, S. K. Y., & Lapusta, N. (2016). Repeating microearthquake sequences interact
752 predominantly through postseismic slip. *Nature Communications*, 7, 13020.
753 doi: 10.1038/ncomms13020
- 754 Marone, C., Vidale, J. E., & Ellsworth, W. L. (1995). Fault healing inferred from
755 time dependent variations in source properties of repeating earthquakes. *Geo-*
756 *physical Research Letters*, 22(22), 3095–3098.
- 757 Materna, K., Taira, T., & Bürgmann, R. (2018). Aseismic transform fault slip at the
758 mendocino triple junction from characteristically repeating earthquakes. *Geo-*
759 *physical Research Letters*, 45(2), 699–707. Retrieved from [https://agupubs](https://agupubs.onlinelibrary.wiley.com/doi/abs/10.1002/2017GL075899)
760 [.onlinelibrary.wiley.com/doi/abs/10.1002/2017GL075899](https://doi.org/10.1002/2017GL075899) doi: [https://](https://doi.org/10.1002/2017GL075899)
761 doi.org/10.1002/2017GL075899
- 762 Mavrommatis, A. P., Segall, P., Uchida, N., & Johnson, K. M. (2015). Long-term
763 acceleration of aseismic slip preceding the Mw 9 Tohoku-oki earthquake: Con-
764 straints from repeating earthquakes. *Geophysical Research Letters*, 42(22),
765 9717–9725.
- 766 Mesimeri, M., & Karakostas, V. (2018). Repeating earthquakes in western corinth
767 gulf (greece): implications for aseismic slip near locked faults. *Geophysical*
768 *Journal International*, 215(1), 659–676.
- 769 Mountjoy, J. J., & Barnes, P. M. (2011). Active upper plate thrust faulting in
770 regions of low plate interface coupling, repeated slow slip events, and coastal
771 uplift: Example from the Hikurangi Margin, New Zealand. *Geochemistry,*

- 772 *Geophysics, Geosystems*, 12(1).
- 773 Nadeau, R. M., Antolik, M., Johnson, P. A., Foxall, W., & McEvelly, T. V. (1994).
 774 Seismological studies at Parkfield III: Microearthquake clusters in the study of
 775 fault-zone dynamics. *Bulletin of the Seismological Society of America*, 84(2),
 776 247–263.
- 777 Nadeau, R. M., Foxall, W., & McEvelly, T. V. (1995). Clustering and periodic re-
 778 currence of microearthquakes on the San Andreas fault at Parkfield, California.
 779 *Science*, 267(5197), 503–507.
- 780 Nadeau, R. M., & Johnson, L. R. (1998). Seismological studies at Parkfield VI:
 781 Moment release rates and estimates of source parameters for small repeating
 782 earthquakes. *Bulletin of the Seismological Society of America*, 88(3), 790–814.
- 783 Nadeau, R. M., & McEvelly, T. V. (1999). Fault slip rates at depth from recurrence
 784 intervals of repeating microearthquakes. *Science*, 285(5428), 718–721.
- 785 Naoi, M., Nakatani, M., Igarashi, T., Otsuki, K., Yabe, Y., Kgarume, T., . . . Ward,
 786 A. (2015). Unexpectedly frequent occurrence of very small repeating earth-
 787 quakes ($-5.1 \leq MW \leq -3.6$) in a South African gold mine: implications for
 788 monitoring intraplate faults. *Journal of Geophysical Research: Solid Earth*,
 789 120(12), 8478–8493.
- 790 Nicol, A., & Wallace, L. M. (2007). Temporal stability of deformation rates: Com-
 791 parison of geological and geodetic observations, Hikurangi subduction margin,
 792 New Zealand. *Earth and Planetary Science Letters*, 258(3-4), 397–413.
- 793 Nomura, S., Ogata, Y., Uchida, N., & Matsu'ura, M. (2017). Spatiotemporal vari-
 794 ations of interplate slip rates in northeast Japan inverted from recurrence
 795 intervals of repeating earthquakes. *Geophysical Journal International*, 208(1),
 796 468–481.
- 797 Passelègue, F. X., Almakari, M., Dublanchet, P., Barras, F., Fortin, J., & Violay,
 798 M. (2020). Initial effective stress controls the nature of earthquakes. *Nature*
 799 *Communications*, 11(1), 1–8.
- 800 Peng, Z., Vidale, J. E., Marone, C., & Rubin, A. (2005). Systematic variations in
 801 recurrence interval and moment of repeating aftershocks. *Geophysical Research*
 802 *Letters*, 32(15), 1–4.
- 803 Reasenber, P. A. (1985). FPFIT, FPLOT, and FPPAGE: Fortran computer pro-
 804 grams for calculating and displaying earthquake fault-plane solutions. *US Geol.*
 805 *Surv. Open-File Rep.*, 85–739.
- 806 Schaff, D. P., & Richards, P. G. (2004). Repeating seismic events in China. *Science*,
 807 303(5661), 1176–1178.
- 808 Schaff, D. P., & Richards, P. G. (2011). On finding and using repeating seismic
 809 events in and near China. *Journal of Geophysical Research: Solid Earth*,
 810 116(B3), 1–20.
- 811 Schaff, D. P., & Richards, P. G. (2014). Improvements in magnitude precision, using
 812 the statistics of relative amplitudes measured by cross correlation. *Geophysical*
 813 *Journal International*, 197(1), 335–350.
- 814 Senobari, N. S., & Funning, G. J. (2019). Widespread fault creep in the northern
 815 San Francisco Bay Area revealed by multistation cluster detection of repeating
 816 earthquakes. *Geophysical Research Letters*, 46(12), 6425–6434.
- 817 Shaddock, H. R., & Schwartz, S. Y. (2019). Subducted seamount diverts shallow slow
 818 slip to the forearc of the northern Hikurangi subduction zone, New Zealand.
 819 *Geology*, 47(5), 415–418.
- 820 Thomas, A. M., Beroza, G. C., & Shelly, D. R. (2016). Constraints on the source pa-
 821 rameters of low-frequency earthquakes on the San Andreas Fault. *Geophysical*
 822 *Research Letters*, 43(4), 1464–1471.
- 823 Todd, E. K., & Schwartz, S. Y. (2016). Tectonic tremor along the northern Hiku-
 824 rangi Margin, New Zealand, between 2010 and 2015. *Journal of Geophysical*
 825 *Research: Solid Earth*, 121(12), 8706–8719.
- 826 Todd, E. K., Schwartz, S. Y., Mochizuki, K., Wallace, L. M., Sheehan, A. F., Webb,

- 827 S. C., ... Fry, B. (2018). Earthquakes and tremor linked to seamount subduc-
 828 tion during shallow slow slip at the Hikurangi Margin, New Zealand. *Journal*
 829 *of Geophysical Research: Solid Earth*, *123*(8), 6769–6783.
- 830 Trugman, D. T., & Shearer, P. M. (2017). GrowClust: A hierarchical clustering
 831 algorithm for relative earthquake relocation, with application to the Spanish
 832 Springs and Sheldon, Nevada, earthquake sequences. *Seismological Research*
 833 *Letters*, *88*(2A), 379–391.
- 834 Uchida, N. (2019). Detection of repeating earthquakes and their application in char-
 835 acterizing slow fault slip. *Progress in Earth and Planetary Science*, *6*(1), 40–
 836 42.
- 837 Uchida, N., & Bürgmann, R. (2019). Repeating earthquakes. *Annual Review of*
 838 *Earth and Planetary Sciences*, *47*, 305–332.
- 839 Uchida, N., Hasegawa, A., Matsuzawa, T., & Igarashi, T. (2004). Pre-and post-
 840 seismic slow slip on the plate boundary off Sanriku, NE Japan associated with
 841 three interplate earthquakes as estimated from small repeating earthquake
 842 data. *Tectonophysics*, *385*(1-4), 1–15.
- 843 Uchida, N., Inuma, T., Nadeau, R. M., Bürgmann, R., & Hino, R. (2016). Periodic
 844 slow slip triggers megathrust zone earthquakes in northeastern Japan. *Science*,
 845 *351*(6272), 488–492.
- 846 Uchida, N., & Matsuzawa, T. (2013). Pre-and postseismic slow slip surrounding
 847 the 2011 Tohoku-oki earthquake rupture. *Earth and Planetary Science Letters*,
 848 *374*, 81–91.
- 849 Uchida, N., Matsuzawa, T., Hasegawa, A., & Igarashi, T. (2003). Interplate quasi-
 850 static slip off Sanriku, NE Japan, estimated from repeating earthquakes. *Geo-*
 851 *physical Research Letters*, *30*(15), 1–4.
- 852 Uchida, N., Matsuzawa, T., Hirahara, S., & Hasegawa, A. (2006). Small repeating
 853 earthquakes and interplate creep around the 2005 Miyagi-oki earthquake (M=
 854 7.2). *Earth, planets and space*, *58*(12), 1577–1580.
- 855 Virtanen, P., Gommers, R., Oliphant, T. E., Haberland, M., Reddy, T., Cournapeau,
 856 D., ... SciPy 1.0 Contributors (2020). SciPy 1.0: Fundamental Algorithms
 857 for Scientific Computing in Python. *Nature Methods*, *17*, 261–272. doi:
 858 10.1038/s41592-019-0686-2
- 859 Wallace, L. M. (2020). Slow Slip Events in New Zealand. *Annual Review of Earth*
 860 *and Planetary Sciences*, *48*, 1–8.
- 861 Wallace, L. M., & Beavan, J. (2010). Diverse slow slip behavior at the Hikurangi
 862 subduction margin, New Zealand. *Journal of Geophysical Research*, *115*(B12),
 863 1–20.
- 864 Wallace, L. M., Beavan, J., Bannister, S., & Williams, C. (2012). Simultaneous
 865 long-term and short-term slow slip events at the Hikurangi subduction margin,
 866 New Zealand: Implications for processes that control slow slip event occur-
 867 rence, duration, and migration. *Journal of Geophysical Research: Solid Earth*,
 868 *117*(B11), 1–18.
- 869 Wallace, L. M., Beavan, J., McCaffrey, R., & Darby, D. (2004). Subduction zone
 870 coupling and tectonic block rotations in the North Island, New Zealand. *Jour-*
 871 *nal of Geophysical Research: Solid Earth*, *109*(B12), 1–21.
- 872 Wallace, L. M., & Eberhart-Phillips, D. (2013). Newly observed, deep slow
 873 slip events at the central Hikurangi margin, New Zealand: Implications for
 874 downdip variability of slow slip and tremor, and relationship to seismic struc-
 875 ture. *Geophysical Research Letters*, *40*(20), 5393–5398.
- 876 Wallace, L. M., Hreinsdóttir, S., Ellis, S., Hamling, I., D’Anastasio, E., & Denys, P.
 877 (2018). Triggered slow slip and afterslip on the southern Hikurangi subduction
 878 zone following the Kaikōura earthquake. *Geophysical Research Letters*, *45*(10),
 879 4710–4718.
- 880 Wallace, L. M., Reyners, M., Cochran, U., Bannister, S., Barnes, P. M., Berryman,
 881 K., ... Ellis, S. (2009). Characterizing the seismogenic zone of a major plate

- 882 boundary subduction thrust: Hikurangi Margin, New Zealand. *Geochemistry,*
 883 *Geophysics, Geosystems*, 10(10), 1–32.
- 884 Wallace, L. M., Webb, S. C., Ito, Y., Mochizuki, K., Hino, R., Henrys, S., ... Shee-
 885 han, A. F. (2016). Slow slip near the trench at the Hikurangi subduction zone,
 886 New Zealand. *Science*, 352(6286), 701–704.
- 887 Warren-Smith, E., Fry, B., Kaneko, Y., & Chamberlain, C. J. (2018). Foreshocks
 888 and delayed triggering of the 2016 MW7. 1 Te Araroa earthquake and dynamic
 889 reinvigoration of its aftershock sequence by the MW7. 8 Kaikōura earthquake,
 890 New Zealand. *Earth and Planetary Science Letters*, 482, 265–276.
- 891 Warren-Smith, E., Fry, B., Wallace, L., Chon, E., Henrys, S., Sheehan, A., ... Lebe-
 892 dev, S. (2019). Episodic stress and fluid pressure cycling in subducting oceanic
 893 crust during slow slip. *Nature Geoscience*, 12(6), 475–481.
- 894 Wessel, P., Luis, J. F., Uieda, L., Scharroo, R., Wobbe, F., Smith, W. H. F., & Tian,
 895 D. (2019). The generic mapping tools version 6. *Geochemistry, Geophysics,*
 896 *Geosystems*, 20(11), 5556–5564.
- 897 Wiemer, S., & Wyss, M. (2000). Minimum magnitude of completeness in earthquake
 898 catalogs: Examples from Alaska, the western United States, and Japan. *Bul-*
 899 *letin of the Seismological Society of America*, 90(4), 859–869.
- 900 Williams, C. A., Eberhart-Phillips, D., Bannister, S., Barker, D. H. N., Henrys, S.,
 901 Reyners, M., & Sutherland, R. (2013). Revised interface geometry for the
 902 Hikurangi subduction zone, New Zealand. *Seismological Research Letters*,
 903 84(6), 1066–1073.
- 904 Williams, J. R., Hawthorne, J. C., & Lengliné, O. (2019). The long recurrence inter-
 905 vals of small repeating earthquakes may be due to the slow slip rates of small
 906 fault strands. *Geophysical Research Letters*, 46(22), 12823–12832.
- 907 Wu, C., Gombert, J., Ben-Naim, E., & Johnson, P. (2014). Triggering of repeating
 908 earthquakes in central California. *Geophysical Research Letters*, 41(5), 1499–
 909 1505.
- 910 Yamashita, Y., Shimizu, H., & Goto, K. (2012). Small repeating earthquake ac-
 911 tivity, interplate quasi-static slip, and interplate coupling in the Hyuga-nada,
 912 southwestern Japan subduction zone. *Geophysical Research Letters*, 39(8),
 913 1–5.
- 914 Yao, D., Walter, J. I., Meng, X., Hobbs, T. E., Peng, Z., Newman, A. V., ... Protti,
 915 M. (2017). Detailed spatiotemporal evolution of microseismicity and repeat-
 916 ing earthquakes following the 2012 Mw 7.6 Nicoya earthquake. *Journal of*
 917 *Geophysical Research: Solid Earth*, 122(1), 524–542.
- 918 Yarce, J., Sheehan, A. F., Nakai, J. S., Schwartz, S. Y., Mochizuki, K., Savage,
 919 M. K., ... Ito, Y. (2019). Seismicity at the northern Hikurangi Margin, New
 920 Zealand, and investigation of the potential spatial and temporal relationships
 921 with a shallow slow slip event. *Journal of Geophysical Research: Solid Earth*,
 922 124(1), 4751–4766.
- 923 Yu, W. (2013). Shallow-focus repeating earthquakes in the
 924 Tonga–Kermadec–Vanuatu subduction zones. *Bulletin of the Seismological*
 925 *Society of America*, 103(1), 463–486.
- 926 Zhang, J., Richards, P. G., & Schaff, D. P. (2008). Wide-scale detection of earth-
 927 quake waveform doublets and further evidence for inner core super-rotation.
 928 *Geophysical Journal International*, 174(3), 993–1006.

Table 1. Summary of the repeating earthquake families identified in each of the regions. Geographic areas are identified in Figure 2, and abbreviations how each of the families are identified. T_{min} and T_{max} are the minimum and maximum recurrence intervals respectively for each of the regional groups. M_{min} and M_{max} are the minimum and maximum local magnitudes respectively for each of the regional groups.

Geographic area	Abbreviation	Number of families	T_{min}	T_{max}	M_{min}	M_{max}
Waihau	WA	1	12.3	12.3	5.2	5.3
Te Araroa	TA	1	6.6	6.6	2.3	2.5
Ruatōria	RA	2	1.9	2.0	2.3	2.6
Te Puia	TP	4	0.0	10.3	2.3	3.5
Tokomaru-Tolaga	TT	34	0.0	11.8	0.6	4.5
Whatatutu	WH	1	4.4	4.4	2.3	2.4
Tolaga South	TS	1	2.0	2.0	2.2	2.5
Te Karaka	TK	7	2.2	8.0	2.0	4.1
Pouawa	PO	5	2.1	7.8	2.1	3.4
Māhia	MA	4	1.7	6.1	2.1	2.6
Nūhaka	NU	2	1.3	1.8	1.6	2.3

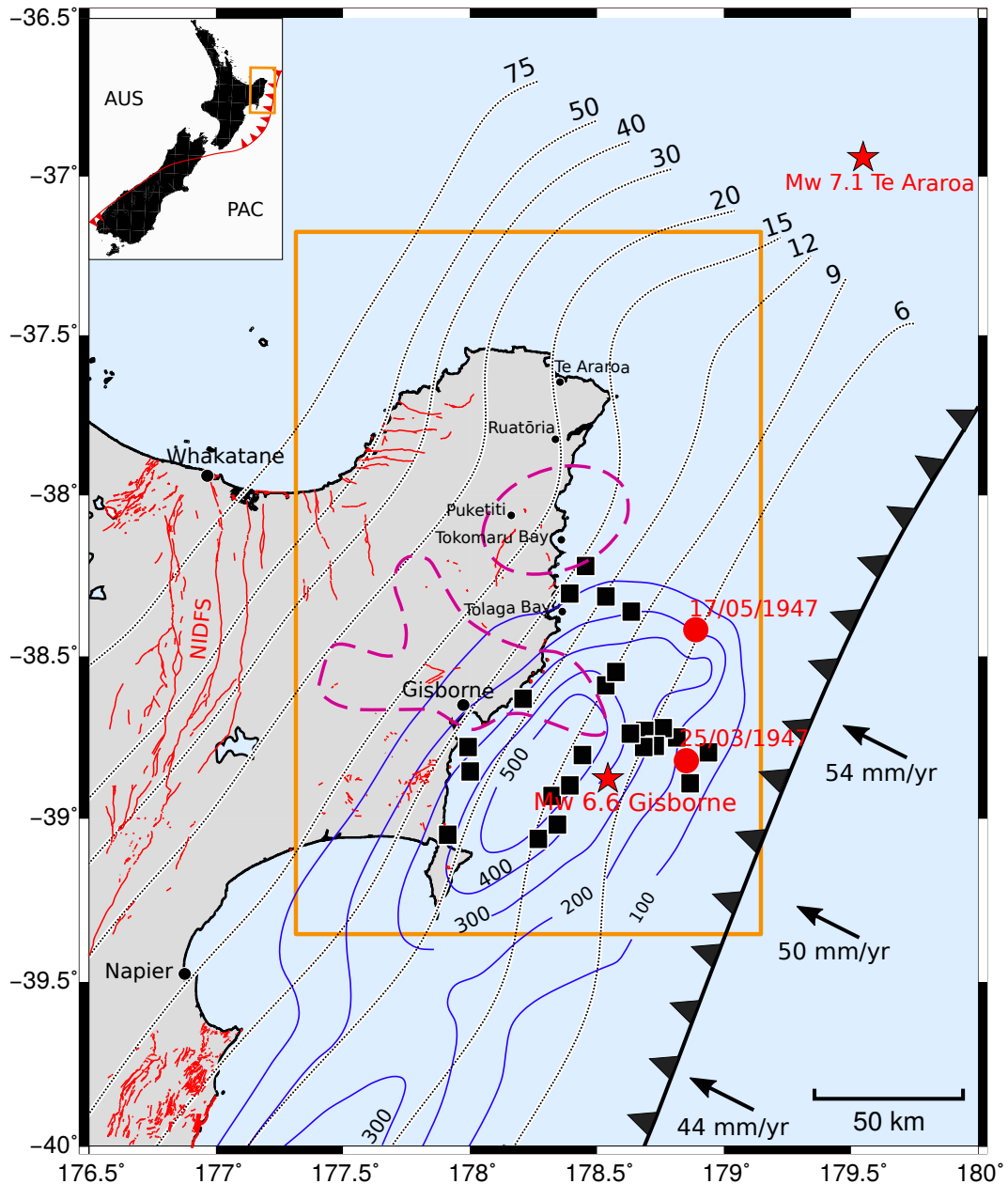


Figure 1. Seismic and aseismic phenomena recorded around the Raukumara Peninsula. Black arrows represent the convergence rates at the trench (Wallace et al., 2012) and black dotted lines represent the depth (labeled in km) to the plate interface (C. A. Williams et al., 2013). Red stars mark the locations of the M_W 6.6 Gisborne earthquake of 2007 and the M_W 7.1 Te Araroa earthquake of 2016. Red circles represent the location of two tsunami-generating earthquakes that occurred in 1947 (Bell et al., 2010). Filled black boxes mark the locations of burst-type repeating earthquakes between May 2014 and July 2015 that were reported by Shaddox and Schwartz (2019). Purple dashed contours demarcate locations of tremor between 2010 and 2015 identified by Todd and Schwartz (2016). Blue contours represent the cumulative slow slip, in mm, that occurred between 2002 and 2014, as described by Wallace (2020). The orange box in the main panel indicates the focus area of this study. Red lines represent active faults from the New Zealand Active Fault Database (Langridge et al., 2016), including the North Island Dextral Fault System (NIDFS). Inset: Map of New Zealand showing the study area in a larger context.

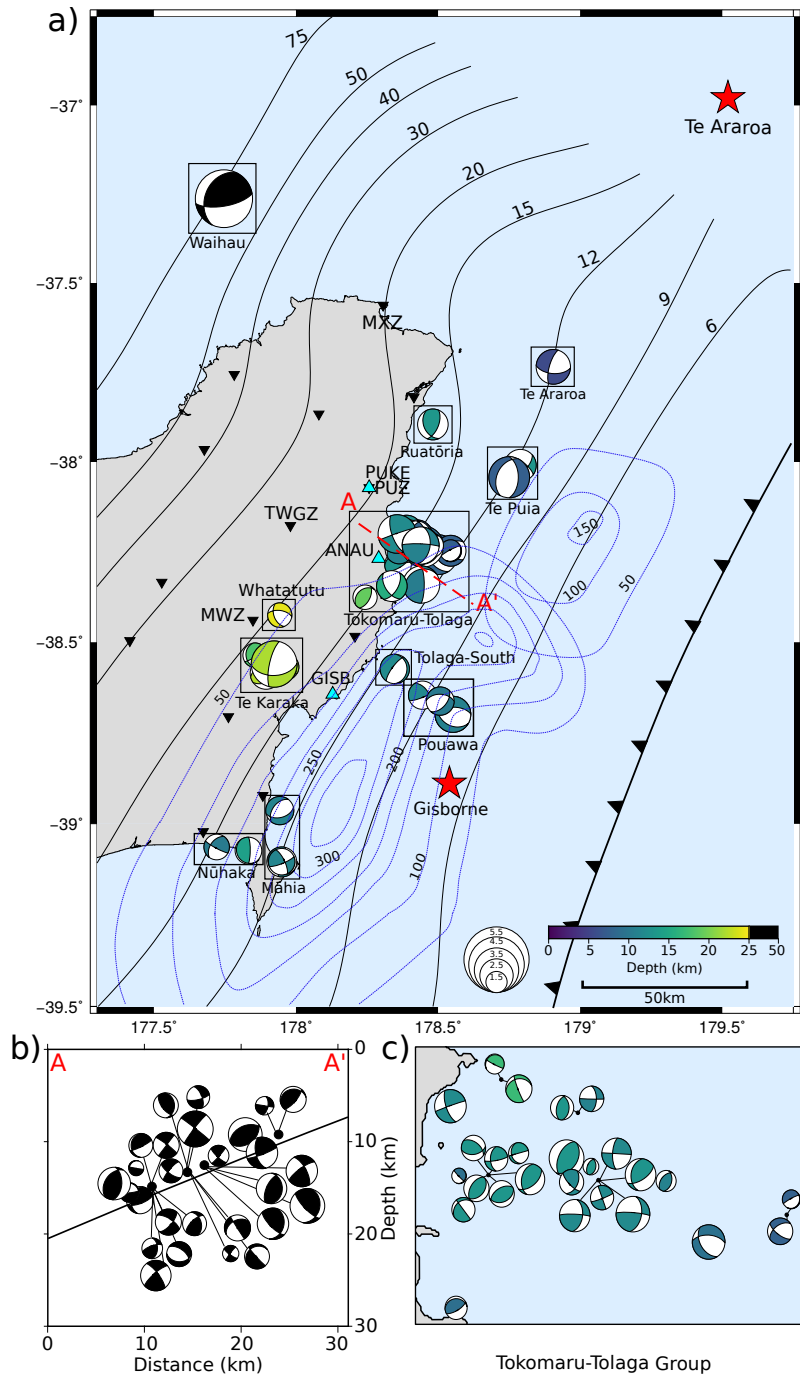


Figure 2. Maps (panels a and c) and cross-section (panel b) of repeating earthquake focal mechanisms. a) The repeating earthquakes are colored by depth and scaled by the calculated magnitudes. The red dashed line labeled A–A' represents the location of the cross-section in b). Contours mark the depth to the subduction interface modeled by C. A. Williams et al. (2013). Black inverted triangles mark the GeoNet seismic stations used to calculate the hypocenter locations. Data from the labeled stations are plotted in Figure 3. Blue contours demarcate slow-slip patches identified by Wallace and Beavan (2010) and Koulali et al. (2017) and are labeled in mm. Red stars mark the locations of the Gisborne $M_W 6.6$ earthquake and the Te Araroa $M_W 7.1$ earthquake. b) Cross-section of the line A–A', displaying seismicity with a ± 10 km swath. c) Expanded view of the Tokomaru-Tolaga group families focal mechanism locations. Note: the maps in a) and c) shows lower hemisphere projections and the cross-section in b) shows back hemisphere projections.

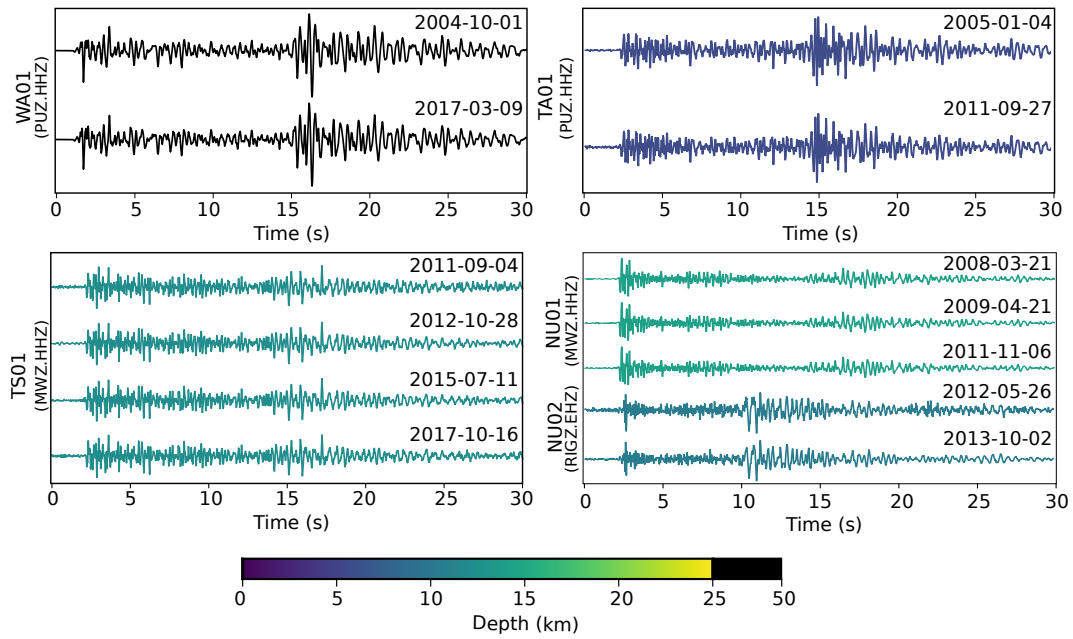


Figure 3. Representative repeating earthquake waveforms from four regional groups. All waveforms have had a fourth-order bandpass filter between 1 and 20 Hz applied. The GeoNet stations and channels that the waveforms were recorded on are included in the brackets under the family names. Waveforms are colored by earthquake depth. Top left: Waihou (WA) group family. Te Puia (TP) group families. Top right: Te Araroa (TA) group family. Bottom left: Tolaga-South (TS) group family. Bottom right: Nūhaka (NU) group families.

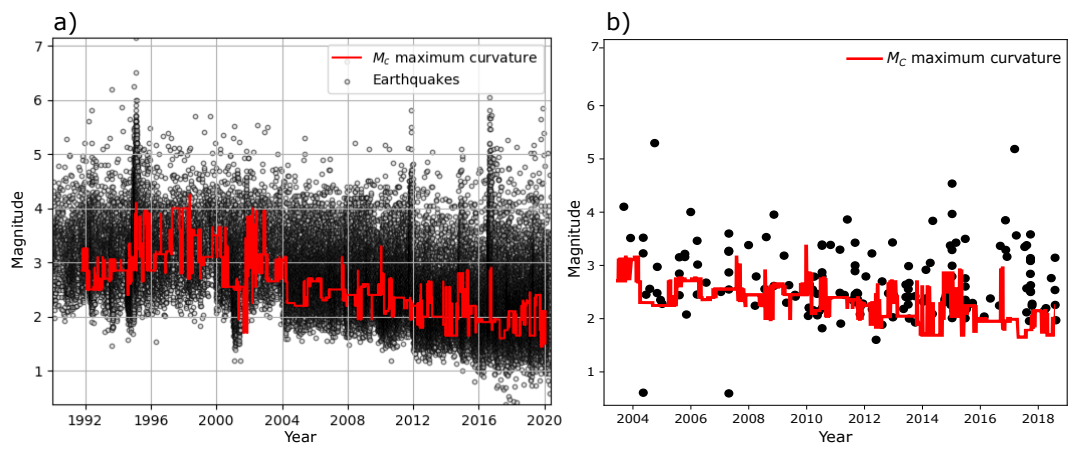


Figure 4. Magnitude of completeness for the repeating earthquake catalog. a) Calculated magnitude of completeness of the GeoNet catalog around the Raukumara region, from 1992 to 2019. We calculated completeness using the maximum curvature method (Wiemer & Wyss, 2000) for groups of 2000 events. b) Calculated local magnitude of the repeating earthquakes identified in this catalog through time. Note the shortened time scale in panel b).

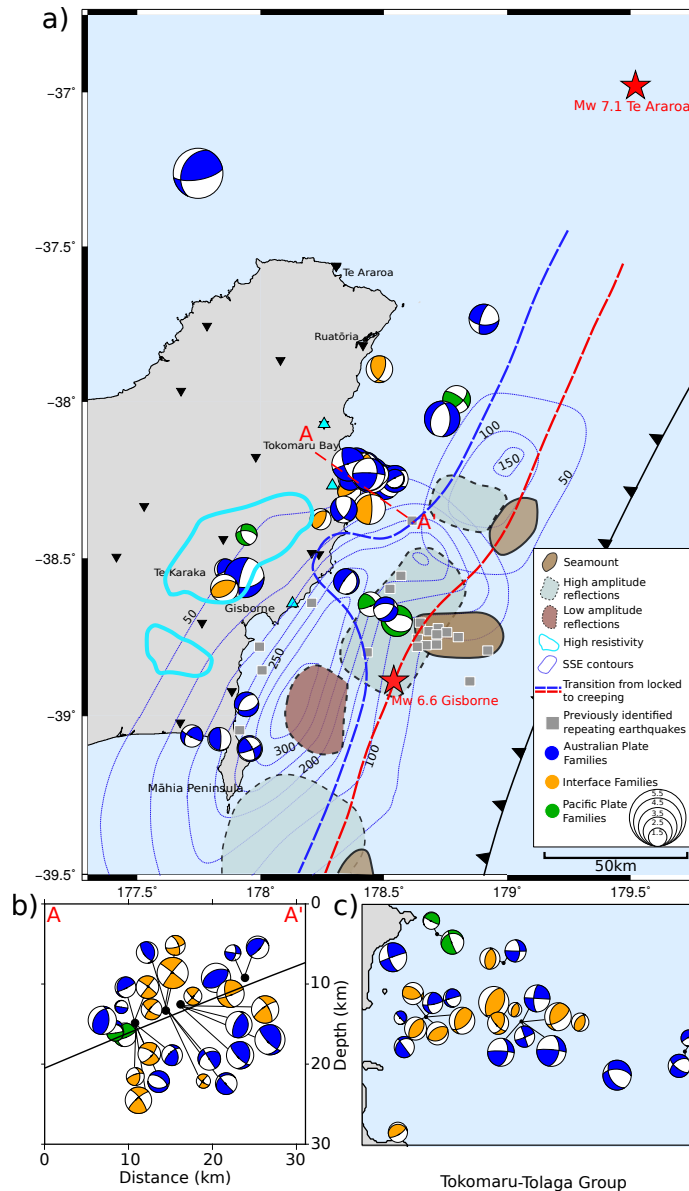


Figure 5. Maps (panels a and c) and cross-section (panel b) of repeating earthquake tectonic locations. a) Locations of the Raukumara Peninsula repeating earthquake families colored according to whether an event is occurring in the Australian Plate, along the interface or within the Pacific Plate, and scaled by calculated magnitude. The red dashed line labeled A–A’ represents the location of the cross-section in b). Blue contours demarcate slow-slip patches identified by Wallace and Beavan (2010) and Koulali et al. (2017) and are labeled in mm. Blue and red dashed lines identify the transition from locked to creeping regions of the geodetic locking model of Wallace et al. (2012). The interface is locked to the right of the red line and creeping to the left of the blue line. Seamount locations and high- and low-amplitude reflections are adapted from Bell et al. (2010), and the regions of the interface which have a high resistivity (200–600 Ωm) are illustrated after Heise et al. (2017). “Burst-type” repeating earthquakes identified by Shaddock and Schwartz (2019) are shown in gray squares. Red stars mark the locations of the Gisborne M_W 6.6 earthquake and the Te Araroa M_W 7.1 earthquake. b) Cross-section of the line A–A’, displaying seismicity with a ± 10 km swath. c) Expanded view of the Tokomaru-Tolaga group families focal mechanism locations. Note: the maps in a) and c) shows lower hemisphere projections and the cross-section in b) shows back hemisphere projections.

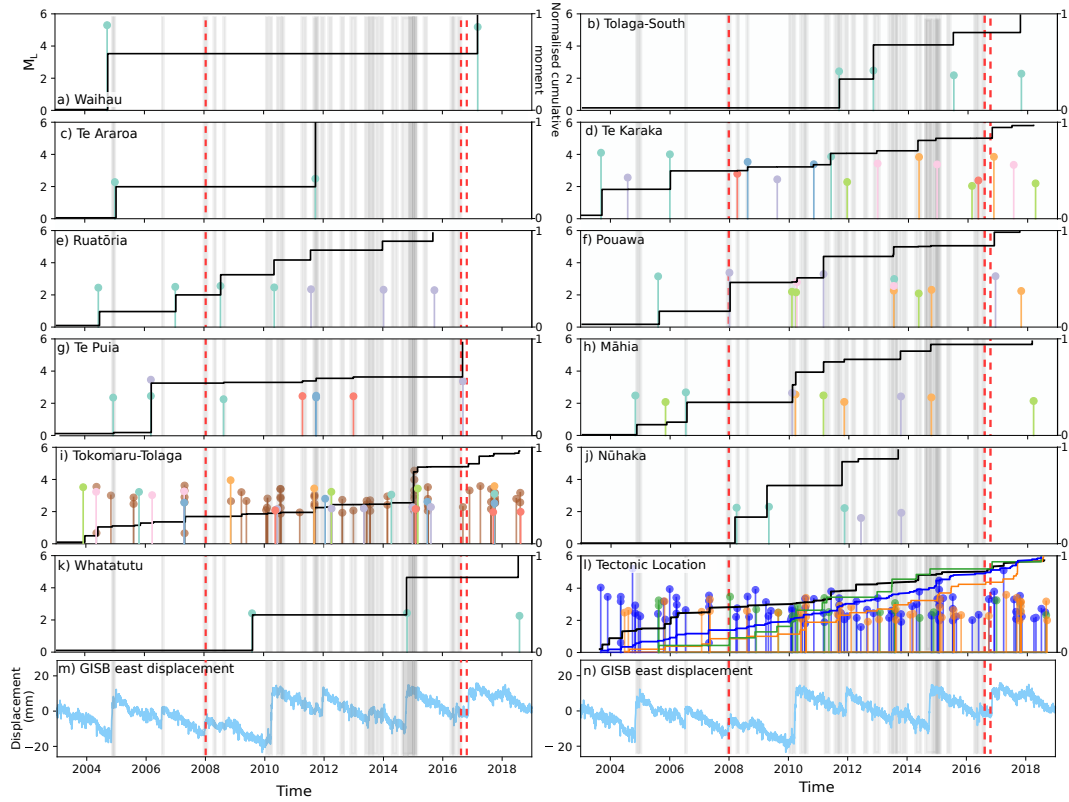
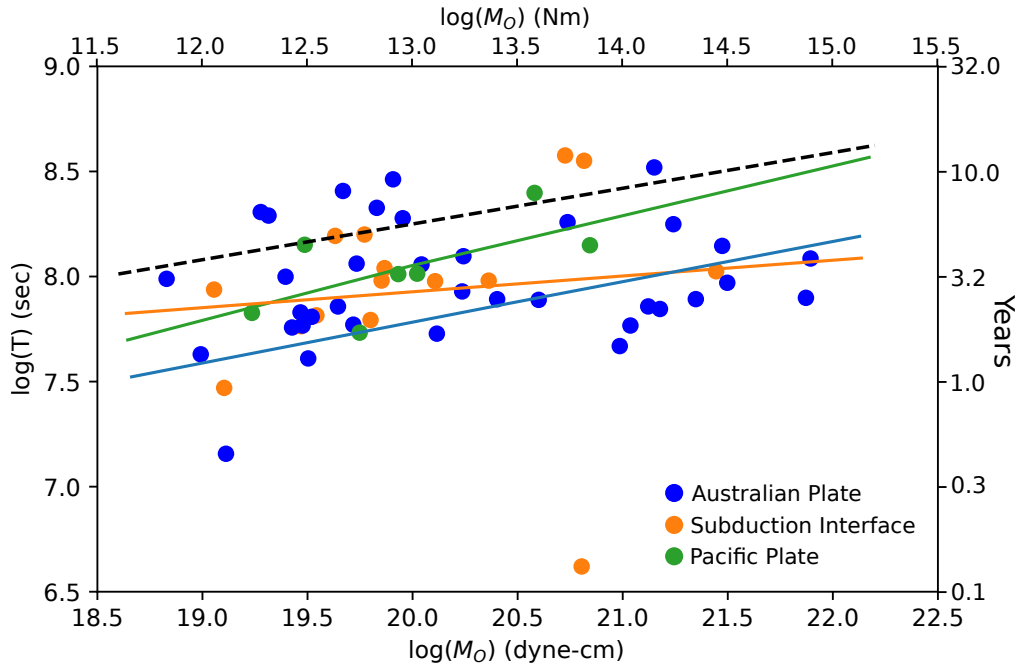


Figure 6. Chronology of repeating earthquakes and cumulative moment release within each geographic area. The lollipop symbols indicate the timing and magnitude of each repeating earthquake and are colored by family. Panel l) depicts the timing of every repeating earthquake colored by their tectonic location (blue is Australian Plate, orange is interface and green is Pacific Plate) and the respective cumulative moment release, while the black line represents the total cumulative moment release. Episodes of slow slip periods (Koulali et al., 2017; Todd & Schwartz, 2016; Wallace & Beavan, 2010; Wallace et al., 2012; Wallace & Eberhart-Phillips, 2013; Wallace et al., 2016) are shown in gray and large earthquakes are marked in red. Note that the slow-slip catalog completeness is not consistent in time. The panels m) and n) show the east-component from the GISB (Gisborne) GNSS site operated by GeoNet and are repeated to aid visual comparisons. The cumulative moment curves are normalized to unity for comparison between different regional groups.



Location	Intercept	Gradient
Australian Plate	3.92 (0.31 - 7.51)	0.19 (0.01 - 0.37)
Interface	6.47 (2.47 - 10.47)	0.07 (-0.13 - 0.27)
Pacific Plate	3.11 (-0.89 - 7.11)	0.25 (0.03 - 0.47)
Nadeau and Johnson (1998): Parkfield	4.85 ± 0.16	0.17 ± 0.009

Figure 7. Repeating earthquake recurrence interval–seismic moment relationship. Top: Raukumara Peninsula repeating earthquake families’ average recurrence interval plotted against seismic moment and colored according to occurrence in the overlying Australian Plate, on the subduction interface or in the subducting Pacific Plate. Shown in the black dashed line is the relationship obtained for repeating earthquakes near Parkfield, California, by Nadeau and Johnson (1998). Linear relationships of the logarithms of each of the variables were fitted by minimizing the L2 norm, after families with durations shorter than six months had been removed. Bottom: Intercept and gradient values, including the 95% confidence intervals for the recurrence interval seismic moment relationships plotted above. The relationship identified by Nadeau and Johnson (1998) has been included for comparison.